

Effects of Initial Conditions on Oscillatory Flow in an Oscillating Heat Pipe

Zheng Li^{1,2}, Mo Yang¹, Yuwen Zhang^{2*} and Stephen Montgomery-Smith²

¹University of Shanghai for Science and Technology, Shanghai 200093, China

²University of Missouri, Columbia, MO 65211, USA

ABSTRACT

Effects of initial conditions on the oscillatory flow in oscillating heat pipes (OHPs) are investigated numerically. Initial vapor temperature, pressure and liquid displacement are in consideration. Three test cases are solved with different initial condition settings. Liquid displacement and vapor temperature tendencies are compared to find which initial condition lead to the best heat transfer performance in all test cases. Fast Fourier transform is employed to calculate the frequency based on liquid displacement. The results show that initial condition has significant effect on oscillating heat pipe performance and keeping initial condition uniform is an effective way for heat transfer enhancement of the system.

KEY WORDS: Oscillating heat pipe, Initial condition, Random number, Fast Fourier Transform

1. INTRODUCTION

With the IT industry fast growing, there is a need for the high-efficiency electronic cooling applications. Oscillating (or Pulsating) Heat Pipes (OHPs or PHPs) that was invented and patented by Akachi [1] in 1990s provide an effective technique for electronics cooling. OHP is made of a long capillary tube that is bent into many turns and phase changes of the working fluids drive oscillatory flow to transport heat from heating section to cooling sections. In the last two decades, OHP has been investigated experimentally and theoretically by many groups around the world. Several experimental investigations [2, 3] were presented to discuss the fluid flow and heat transfer characteristics in looped OHP. Hosoda et al. [4] investigated the vapor plug in looped OHP numerically by neglecting the thin film between vapor and the tube wall. Qu and Ma [5] analyzed the primary factors affecting the startup characteristics of OHPs.

With this technology developing, the unlooped system was also used in OHP [6]. Maezawa [7] presented the chaotic behaviors in unlooped OHP based on experimental results. Lee et al. [8] reported flow visualization in OHPs to discuss the vapor bubble mechanism. Shafii et al. [9] reported analytical models for both unlooped and looped OHPs. The heat transfers in unlooped and looped OHPs were analyzed using these models [10]. Zhang and Faghri [11] analyzed the oscillatory flow and heat transfer in OHPs with open end. Zhang and Faghri [12] discussed oscillatory flow in OHP with arbitrary numbers of turns. It was concluded that the oscillation amplitude and circular frequency for different liquid slug are slightly different from each other when the number of turns is greater than 5.

Research to better OHPs is still an important topic because a number of advances and unsolved issues still remain in OHPs [13]. Liang and Ma [14] proposed a mathematical model to analyze the slug flow in OHPs. The sensible heat transfer coefficient between the liquid slug and minichannel wall was obtained for laminar and turbulent liquid flow [15]. Shao and Zhang [16] discussed the film evaporation and condensation effects on oscillatory flow and heat transfer in OHPs. Capillary and gravitational forces effects on OHPs performance were also evaluated [17]. The OHP heating and cooling section temperatures were assumed to be constant in many papers while they have fluctuations in reality. The effects of these fluctuations on the performance of OHP were also investigated [18]. Thompson et al. [19] proposed a new type of flat plate OHP allowing multiple heating arrangements and higher fluxes. Nanofluid was applied to OHP to better its performance [20]. Initial

*Corresponding Author: zhangyu@missouri.edu

condition is important in the fluid flow and heat transfer process. Very limited research has been reported to discuss this initial condition effects to OHP. It was assumed in Ref. [12] that all vapor plugs have the same initial temperature and pressure, and all liquid slugs have the same initial displacement. This uniform initial condition is hard to reach in reality. In this paper, the authors compare different initial conditions OHPs characteristics to analyze these effects.

2. PHYSICAL MODEL

Figure 1 shows the physical model of the OHP under consideration.

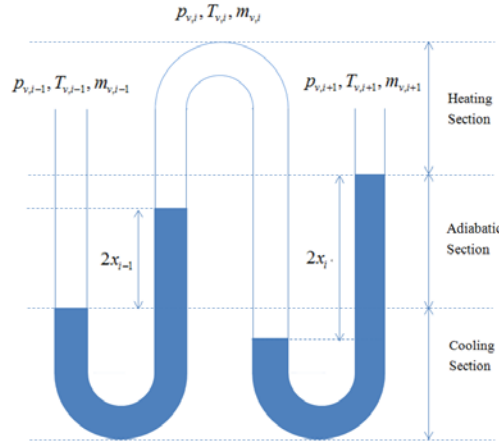


Fig. 1 Physical model

A capillary tube with diameter d is bent into n turns with same length (L) with the two ends are sealed. The heating section (evaporator) has a height of L_h and its wall temperature is kept at T_e . On the other hand, the cooling section (condenser) has a height of L_c and its wall temperature is kept at T_c . There is an adiabatic section with height of L_a between the heating and cooling sections. There is a liquid slug with the same length of $2L_p$ in each turn. The specific liquid slug displacement is represented by x_i . Positive and negative x_i indicate liquid slug moving to right and left, respectively. These liquid slugs also separate different vapor plugs from each other.

2.1 Governing equation

For the vapor plugs in OHP turns, the pressure relates to the temperature with the following equation [12]:

$$p_{v,i} = \frac{4C_i R_g}{\pi d^2} T_{v,i}^{\gamma/(\gamma-1)} \quad (1)$$

where C_i is constant for different vapor plugs. It is decided by the initial vapor pressure $p_{0,i}$ and temperature $T_{0,i}$:

$$C_i = (\pi d^2 / 4 R_g) p_{0,i} T_{0,i}^{-\gamma/(\gamma-1)} \quad (2)$$

The momentum equation for i^{th} liquid slug is:

$$2A_c L_p \rho_l \frac{d^2 x_i}{dt^2} = (p_{v,i} - p_{v,i+1}) A_c - 2\rho_l g A_c x_i - 2\pi d L_p \tau_p \quad (3)$$

The cross sectional area A_c and shear stress τ_p are defined as:

$$A_c = \pi d^2 / 4 \quad (4)$$

$$\tau_p = \frac{8\mu}{d} \frac{dx_i}{dt} \quad (5)$$

Equation (3) can be simplified to:

$$\frac{d^2 x_i}{dt^2} + \frac{32\nu}{d^2} \frac{dx_i}{dt} + \frac{g}{L_p} x_i = \frac{p_{v,i} - p_{v,i+1}}{2L_p \rho_l} \quad (6)$$

Once the vapor pressure is known, x_i can be obtained from the equation above. The vapor mass changes with x_i due to the evaporation and condensation in OHP.

$$\frac{dm_{v,i}}{dt} = \frac{h_e \pi d (T_e - T_{v,i}) (L_{h,L} + L_{h,R})}{h_{fg}} - \frac{h_c \pi d (T_{v,i} - T_c) (L_{c,L} + L_{c,R})}{h_{fg}} \quad (7)$$

where $L_{h,L}$ and $L_{h,R}$ are heating sections in contact with vapor plug while $L_{c,L}$ and $L_{c,R}$ are cooling sections in contact with vapor plug.

$$L_{h,L} = \begin{cases} L - (L_p + x_{i-1}) & L_p + x_{i-1} \geq L_c + L_a \\ 0 & L_p + x_{i-1} < L_c + L_a \end{cases} \quad (8a)$$

$$L_{h,R} = \begin{cases} L - (L_p - x_i) & L_p - x_i \geq L_c + L_a \\ 0 & L_p - x_i < L_c + L_a \end{cases} \quad (8b)$$

$$L_{c,L} = \begin{cases} L_c - (L_p + x_{i-1}) & L_p + x_{i-1} < L_c \\ 0 & L_p + x_{i-1} \geq L_c \end{cases} \quad (8c)$$

$$L_{c,R} = \begin{cases} L_c - (L_p - x_i) & L_p - x_i < L_c \\ 0 & L_p - x_i \geq L_c \end{cases} \quad (8d)$$

Using the ideal gas law, the vapor mass can also be obtained from:

$$m_{v,1} = \frac{\pi d^2}{4R_g T_0} p_{v,1} [(L - L_p) + x_{v,1}] \quad (9a)$$

$$m_{v,i} = \frac{\pi d^2}{4R_g T_0} p_{v,i} [2(L - L_p) + x_{v,i} - x_{v,i-1}], \quad i = 2, 3, \dots, n \quad (9b)$$

$$m_{v,n+1} = \frac{\pi d^2}{4R_g T_0} p_{v,n} [(L - L_p) + x_{v,n}] \quad (9c)$$

2.2 Initial condition

Different initial conditions are employed to investigate their effects to the OHP performance. It is assumed that the initial vapor pressure, temperature and liquid displacement are:

$$p_{0,i} = p_0 + A_1 p_0 (RN_1 - 0.5) \quad (10a)$$

$$T_{0,i} = T_0 + A_2 T_0 (RN_2 - 0.5) \quad (10b)$$

$$x_{0,i} = x_0 + A_3 x_0 (RN_3 - 0.5) \quad (10c)$$

where RN_1 , RN_2 and RN_3 are the random numbers chosen from standard uniform distribution. A_1 , A_2 and A_3 limit the random number ranges, T_0 is a reference temperature that is chosen as the average of T_e and T_c , p_0 is the corresponding pressure at reference state, and x_0 is the mean value of initial displacement. The reference state constant C_0 and mass m_0 are:

$$C_0 = (\pi d^2 / 4R_g) p_0 T_0^{-\gamma/(\gamma-1)} \quad (11a)$$

$$m_0 = \frac{\pi d^2}{2R_g T_0} p_0 (L - L_p) \quad (11b)$$

Then C_i and initial vapor mass can be obtained from these initial conditions:

$$C_i = (\pi d^2 / 4R_g) p_{0,i} T_{0,i}^{-\gamma/(\gamma-1)} \quad (12)$$

$$m_{0,1} = \frac{\pi d^2}{4R_g T_0} p_{0,1} [(L - L_p) + x_{0,1}] \quad (13a)$$

$$m_{0,i} = \frac{\pi d^2}{4R_g T_0} p_{0,i} [2(L - L_p) + x_{0,i} - x_{0,i-1}] \quad (13b)$$

$$m_{0,n+1} = \frac{\pi d^2}{4R_g T_0} p_{0,n} [(L - L_p) + x_{0,n}] \quad (13c)$$

2.3 Non-dimensional governing equations

Defining the following non-dimensional parameters

$$\left\{ \begin{array}{l} \theta_i = \frac{T_{v,i}}{T_0}, P_i = \frac{p_{v,i}}{p_0}, M_i = \frac{m_{v,i}}{m_0}, X_i = \frac{x_i}{x_0}, \varepsilon = \frac{L_p}{L} \\ \tau = \frac{vt}{d^2}, \omega^2 = \frac{gd^4}{L_p v^2}, \zeta = \frac{p_0 d^4}{2\rho_l L_p L_h v^2} \end{array} \right. \quad (14)$$

the governing equations and initial conditions become:

$$\frac{d^2 X_i}{d\tau^2} + 32 \frac{dX_i}{d\tau} + \omega^2 X_i = \zeta (P_i - P_{i+1}) \quad (15)$$

$$\frac{dM_i}{d\tau} = H_e (L_{h,L}^* + L_{h,R}^*) (\theta_e - \theta_i) - H_c (L_{c,L}^* + L_{c,R}^*) (\theta_i - \theta_c) \quad (16)$$

where

$$H_c = \frac{4h_c R_g T_0^2 d}{p_0 h_{fg} \nu}, H_e = \frac{4h_e R_g T_0^2 d}{p_0 h_{fg} \nu}, \theta_c = \frac{T_c}{T_0}, \theta_e = \frac{T_e}{T_0} \quad (17)$$

$$L_{h,L}^* = \begin{cases} 1 - (\varepsilon + X_{i-1}) & \varepsilon + X_{i-1} \geq 1 - L_h^* \\ 0 & \varepsilon + X_{i-1} < 1 - L_h^* \end{cases} \quad (18a)$$

$$L_{h,R}^* = \begin{cases} 1 - (\varepsilon - X_i) & \varepsilon - X_i \geq 1 - L_h^* \\ 0 & \varepsilon - X_i < 1 - L_h^* \end{cases} \quad (18b)$$

$$L_{c,L}^* = \begin{cases} L_c^* - (\varepsilon + X_{i-1}) & \varepsilon + X_{i-1} < L_c^* \\ 0 & \varepsilon + X_{i-1} \geq L_c^* \end{cases} \quad (18c)$$

$$L_{c,R}^* = \begin{cases} L_c^* - (\varepsilon - X_i) & \varepsilon - X_i < L_c^* \\ 0 & \varepsilon - X_i \geq L_c^* \end{cases} \quad (18d)$$

$$M_1 = \theta_1^{1/(\gamma-1)} C_1^R \left[\frac{1}{2} + \frac{X_1}{2(1-\varepsilon)} \right] \quad (19a)$$

$$M_i = \theta_i^{1/(\gamma-1)} C_i^R \left[1 + \frac{X_i - X_{i-1}}{2(1-\varepsilon)} \right] \quad i = 2, 3, \dots, n \quad (19b)$$

$$M_{n+1} = \theta_{n+1}^{1/(\gamma-1)} C_{n+1}^R \left[\frac{1}{2} - \frac{X_n}{2(1-\varepsilon)} \right] \quad (19c)$$

$$P_i = C_i^R (\theta_i)^{\gamma/(\gamma-1)} \quad (19d)$$

where

$$C_i^R = C_i / C_0 \quad (19e)$$

The initial conditions are:

$$P_{0,i} = 1 + A_1 (RN_1 - 0.5) \quad (20a)$$

$$\theta_{0,i} = 1 + A_2 (RN_2 - 0.5) \quad (20b)$$

$$X_{0,i} = 1 + A_3 (RN_3 - 0.5) \quad (20c)$$

3. NUMERICAL PROCEDURE

After the non-dimensional process, the iteration method and implicit difference method are employed to solve the governing equations with initial conditions. OHP working conditions can be simulated by the following steps:

- (1) Set the initial conditions.
- (2) Guess the dimensionless temperature θ_i for all the vapor plugs.
- (3) Calculate the vapor dimensionless pressure P_i using Eq. (19d)
- (4) Calculate the liquid slug dimensionless displacement by Eq. (15).
- (5) Calculate the vapor dimensionless mass M_i using Eq. (16)
- (6) Calculate the vapor dimensionless θ_i by Eqs. (19a) to (19c).
- (7) Compare θ_i in step (6) with that in step (2). If the difference meets the error tolerance, then go to the next step. Or else, use step (6) θ_i result as the new guess dimensionless temperature and repeat steps (2) to (6) till the converged results are reached.

The working fluid oscillates in the tubes when OHP starts working. Its amplitude and circular frequency are considered to evaluate the OHP performance. Oscillation amplitude can be viewed from liquid displacement or vapor temperature directly. Fast Fourier transform (FFT) is employed to calculate the circular frequency [21].

4. RESULTS AND DISCUSSIONS

Initial condition plays an important role in fluid flow and heat transfer problems. Initial vapor temperature, pressure and liquid displacement are in consideration. This article discusses the initial condition effects by adding random numbers to them in Eq. (10). Meanwhile, the initial vapor temperature and pressure show their effects to OHP governing equation in parameter C_i^R in Eq. (19). Three sets of initial conditions: (1) uniform initial condition, $A_1 = A_2 = A_3 = 0$; (2) liquid random initial displacement $A_1 = A_2 = 0, A_3 \neq 0$; and (3) random initial vapor temperature, pressure and liquid displacement $A_1 \neq 0, A_2 \neq 0, A_3 \neq 0$ are applied to the three test cases, respectively. Larger amplitude and higher circular frequency indicate better OHP performance [12]. The initial condition effects are discussed by comparing these results.

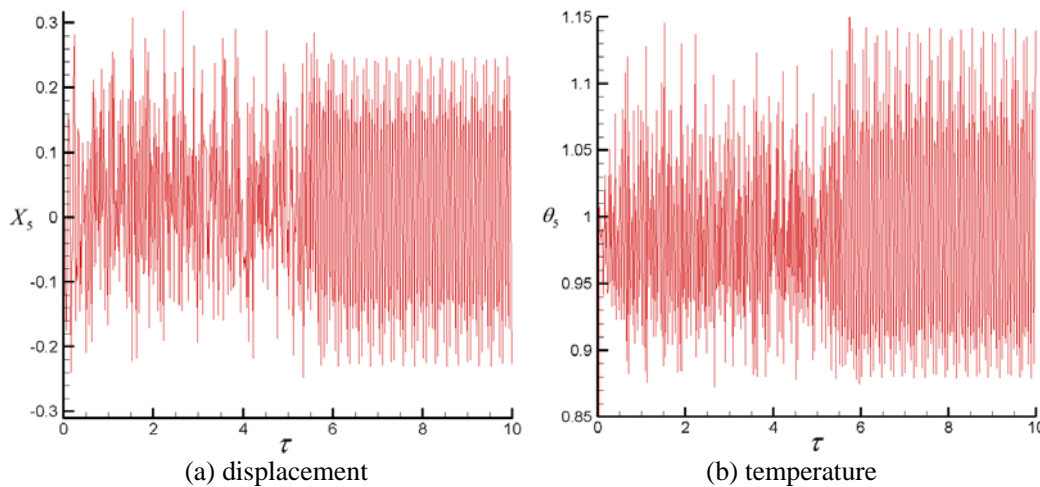


Fig. 2 Liquid slug displacement and vapor temperature ($H_e = H_c = 125, A_1 = A_2 = A_3 = 0$)

Three test cases all have ten turns ($n = 10$). Only 5th vapor slug and 5th liquid plug results are recorded for comparison. It was assumed that $L_h = 0.1\text{m}$, $L_c = 0.1\text{m}$, $L_a = 0$, $L_p = 0.08\text{m}$, $d = 3.34\text{mm}$, $T_c = 90^\circ\text{C}$ and $T_e = 110^\circ\text{C}$ in all the cases. Accordingly, the dimensionless parameters are: $\theta_e = 1.1$, $\theta_c = 0.9$, $\omega^2 = 1.2 \times 10^4$, $\zeta = 1.2 \times 10^5$, $L_h^* = 0.5$, $L_c^* = 0.5$ and $\varepsilon = 0.4$ from the non-dimensional process.

Figure 2 shows displacement of the liquid slug and vapor temperature with uniform initial conditions ($A_1 = A_2 = A_3 = 0$) and both H_e and H_c are 125. The observed liquid displacement oscillates between -0.25 and 0.30 after τ is greater than 6. The observed vapor temperature tendency is similar to that of the liquid slug displacement. Its oscillation indicates the vapor moving between the cooling and heating sections.

Figure 3 shows the liquid slug displacement and vapor temperature with random initial liquid displacements ($A_1 = A_2 = 0, A_3 = 0.15$) while all other conditions are same as those in Fig. 2. The liquid displacement oscillates between -0.25 to 0.25. This amplitude is lower than that of the uniform initial condition case. It also becomes periodic to after τ reaches to 1. The vapor temperature tendency is also periodic after τ equals 1. It indicates that random displacement led to quick and weaker steady oscillations.

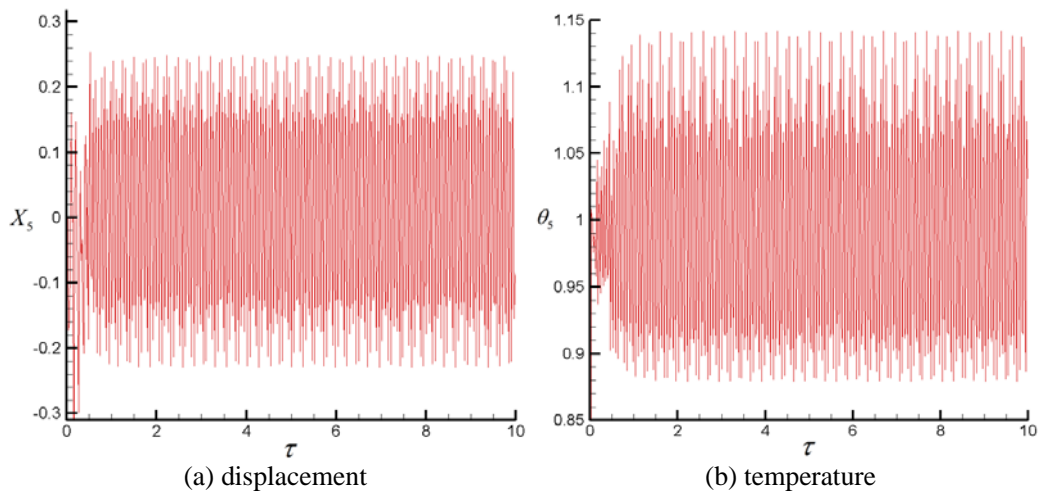


Fig. 3 Liquid slug displacement and vapor temperature ($H_e = H_c = 125, A_1 = 0, A_2 = 0, A_3 = 0.15$)

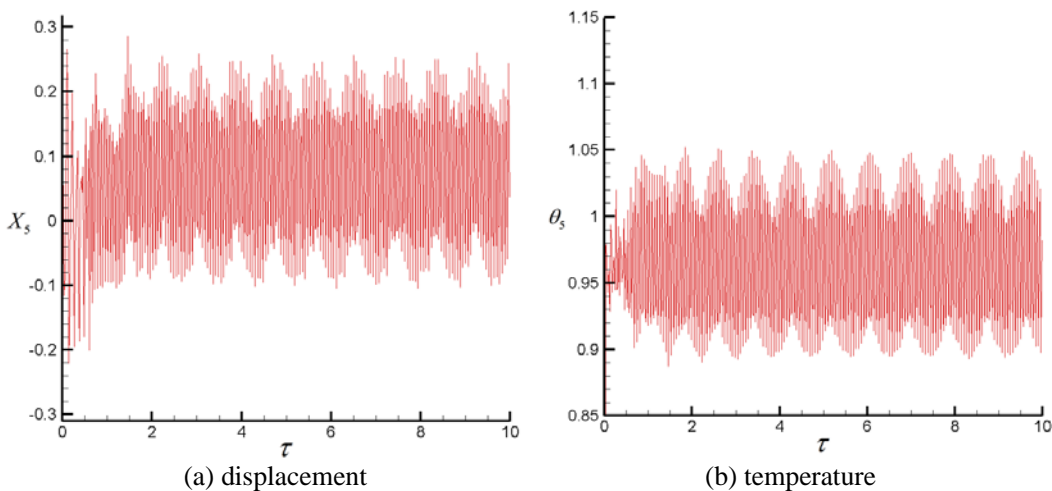


Fig. 4 Liquid slug displacement and vapor temperature ($H_e = H_c = 125, A_1 = A_2 = 0.20, A_3 = 0.15$)

Figure 4 shows liquid slug displacement and vapor temperature with random initial vapor temperature, pressure and liquid displacement ($A_1 = A_2 = 0.20$, $A_3 = 0.15$) while other conditions are same as Fig. 2. It can be seen that the liquid displacement and vapor temperature oscillation amplitude are smaller than those in Figs. 2 and 3. Meanwhile it reaches periodic at the same time as that in Fig. 2. Therefore, the random vapor temperature and pressure decreases the OHP oscillation amplitude and has no apparent effect to the time to reach periodic.

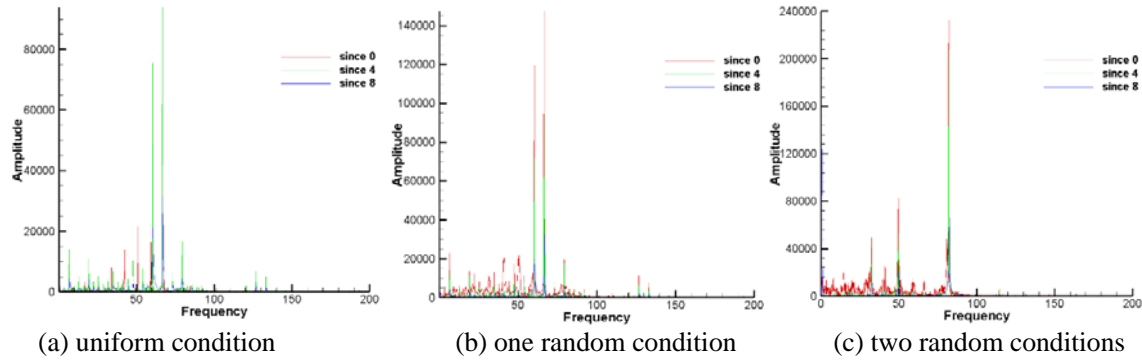


Fig. 5 Comparison of frequencies ($H_e = H_c = 125$)

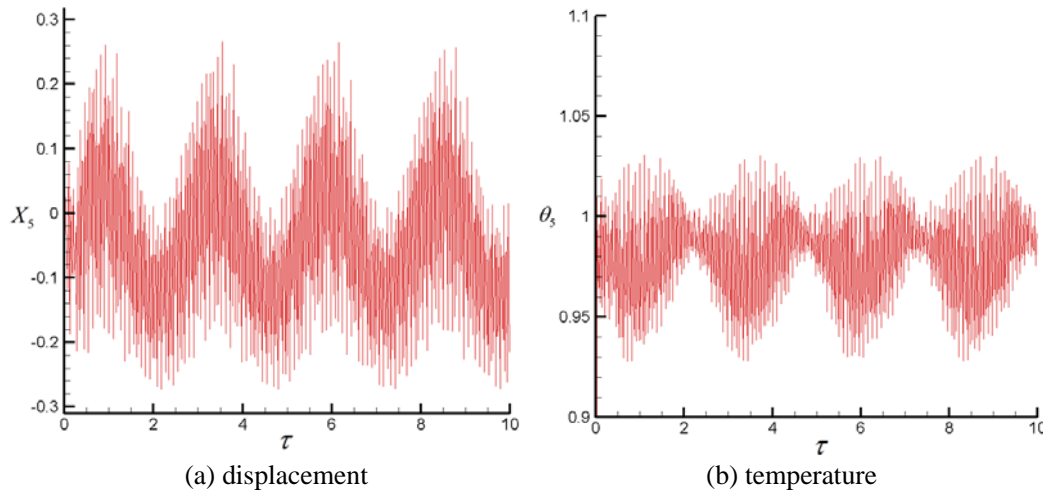


Fig. 6 Liquid slug displacement and vapor temperature ($H_e = H_c = 250$, $A_1 = A_2 = A_3 = 0$)

Figure 5 shows the comparison of frequencies among results at different initial conditions. The FFT results are based on liquid displacement. The one since time equals 8 doesn't have that much noise as the other conditions. It's in consideration because it eliminates the aperiodic results effects at the beginning. For the case with uniform initial condition, three highest frequency picks locate at 67, 60 and 79, respectively. They are independent since their greatest common divisor is 1. Therefore the final oscillation is composed by several independent periodic ones. When the random liquid displacement initial condition is used, three highest frequencies are 68, 59 and 79. The frequency results are slightly different from the ones with uniform initial condition. Taking random initial vapor pressure, temperature and liquid displacement in consideration, the three highest frequencies are 78, 50 and 30, respectively. The composed frequency turns to be lower than those for the previous two cases. Therefore, uniform initial condition and random initial liquid displacement led to a similar circular frequency which is higher than the one using random initial vapor pressure, temperature and liquid displacement.

The effects of H_e and H_c are investigated by increasing their values to 250. Figure 6 shows the liquid slug displacement and vapor temperature with uniform initial condition ($A_1 = A_2 = A_3 = 0$). The liquid displacement

and vapor temperature oscillate round two waves, respectively. The displacement ranges from -0.3 to 0.3 while the temperature changes between 0.93 and 1.03.

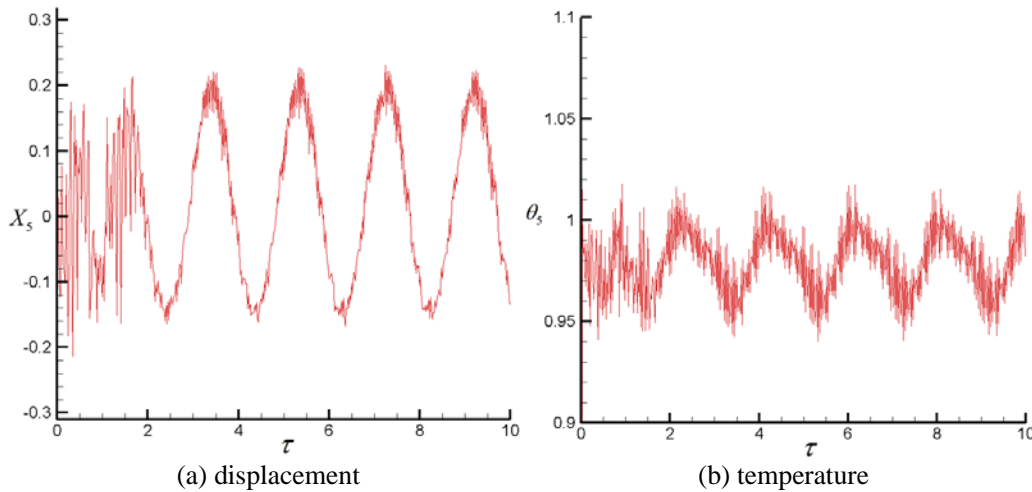


Fig. 7 Liquid slug displacement and vapor temperature ($H_e = H_c = 250$, $A_1 = A_2 = 0$, $A_3 = 0.15$)

Figure 7 is the results with random initial liquid displacement ($A_1 = A_2 = 0$, $A_3 = 0.15$) while other conditions are same as those in Fig. 6. The liquid displacement and vapor temperature also oscillate round two waves respectively. Two amplitudes are both lower than that in the uniform initial condition shown in Fig. 6. The displacement and temperature ranges are also smaller. Therefore the random liquid displacement limits the OHP oscillation amplitude. Figure 8 is the results with random initial vapor temperature, pressure and liquid displacement ($A_1 = A_2 = 0.20$, $A_3 = 0.15$) while other conditions are same as those in Fig. 6. It can be seen that the oscillation is weakest among the results of different initial condition settings because the displacement and temperature ranges are smallest. It also indicates random initial vapor temperature and pressure can lower the OHP oscillation amplitude.

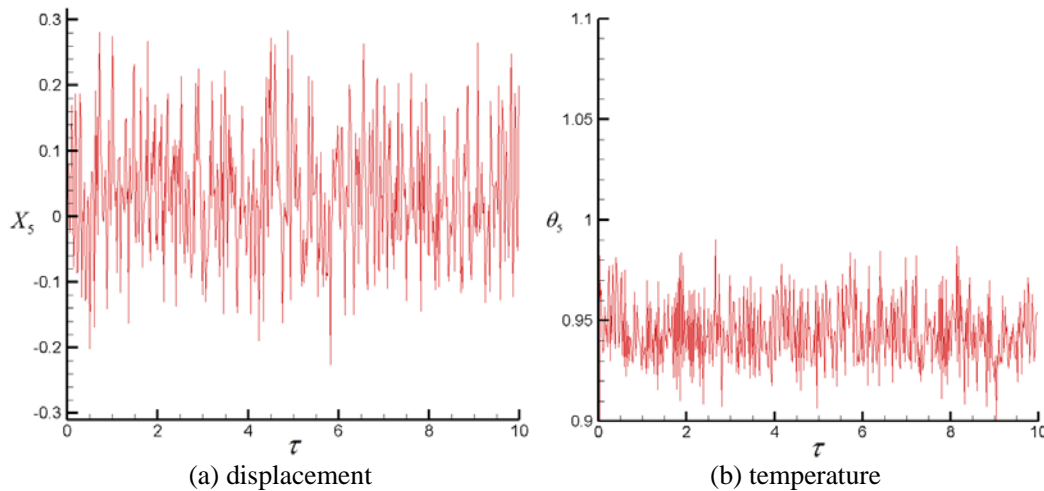


Fig. 8 Liquid slug displacement and vapor temperature ($H_e = H_c = 250$, $A_1 = A_2 = 0.20$, $A_3 = 0.15$)

Figure 9 shows the comparison of frequencies among the three sets of initial conditions for $H_e = H_c = 250$. The one since time equals 8 is in consideration to eliminate the aperiodic results effects at the beginning. The three highest frequencies are respectively 31, 50 and 81, when uniform initial condition is used. If random initial liquid displacement is employed, the top three frequencies are 50, 23 and 28. Quasi-periodic state [22] is reached since 23 and 27 are very close. Many similar strength frequencies under 78 appear when random initial

vapor pressure, temperature and liquid displacement are in consideration. It means that OHP reaches a state combining periodic and chaos results.

Simulation is then carried out for the cases that H_e and H_c are both 500. Figure 10 shows the results with uniform random initial condition ($A_1 = A_2 = A_3 = 0$). The liquid displacement and vapor temperature become periodic after τ equals 2. Then liquid displacement oscillates between -0.1 and 0.2 while vapor temperature ranges from 0.93 to 1.03.

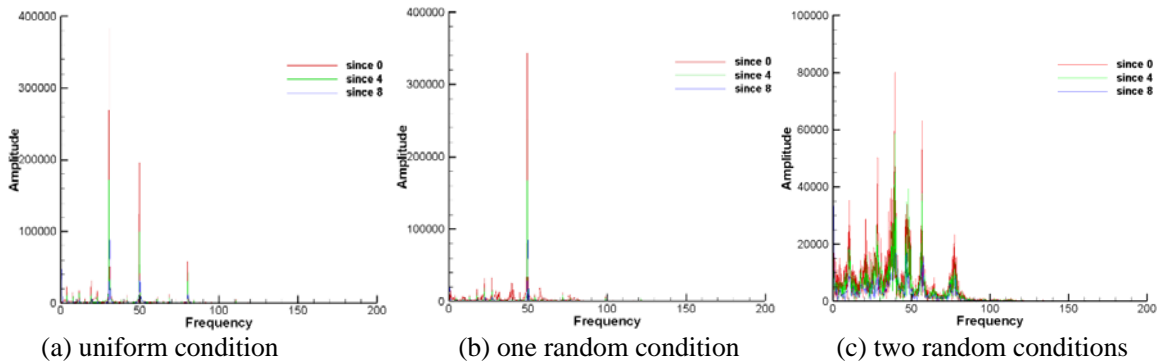


Fig. 9 Comparison of frequencies ($H_e = H_c = 250$)

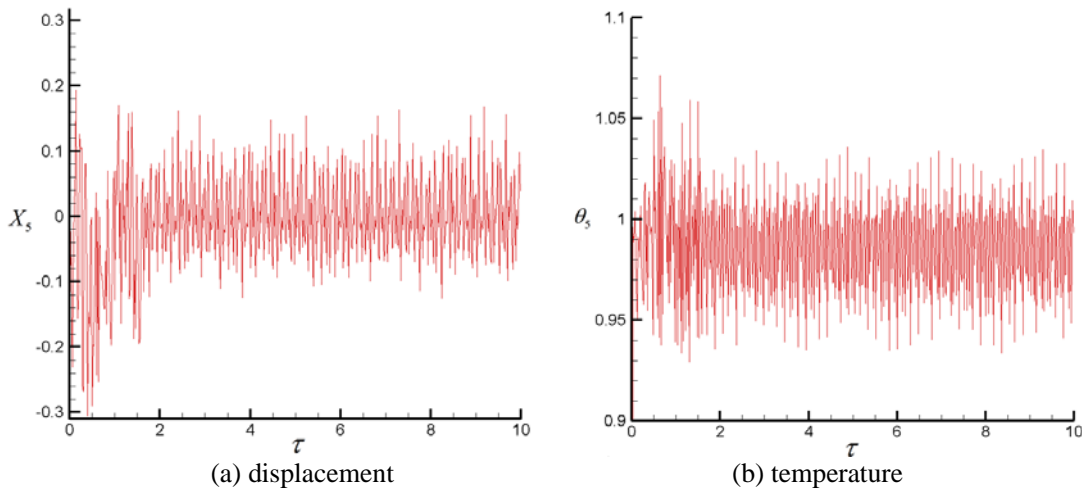


Fig. 10 Liquid slug displacement and vapor temperature ($H_e = H_c = 500$, $A_1 = A_2 = A_3 = 0$)

Figure 11 shows the results with liquid random initial displacement ($A_1 = A_2 = 0$, $A_3 = 0.15$) while other conditions are same as Fig. 10. The liquid displacement and vapor temperature also become periodic after τ equals 2. And their amplitudes are also close to that of the uniform initial condition results. This means that the random liquid displacement effect to OHP is limited for high H_e and H_c . After adding random initial vapor temperature, pressure and liquid displacement ($A_1 = A_2 = 0.20$, $A_3 = 0.15$), the results show valid difference from that in the previous two conditions.

As can be seen from Fig. 12, the liquid displacement oscillates around a wave since τ equals 4. But the displacement is greater than zero for most of the time. It means that the liquid plug does not move to the left that much. This phenomenon may limit the OHP oscillation range. The vapor temperature oscillates between 0.9 and 1.05 after becoming periodic.

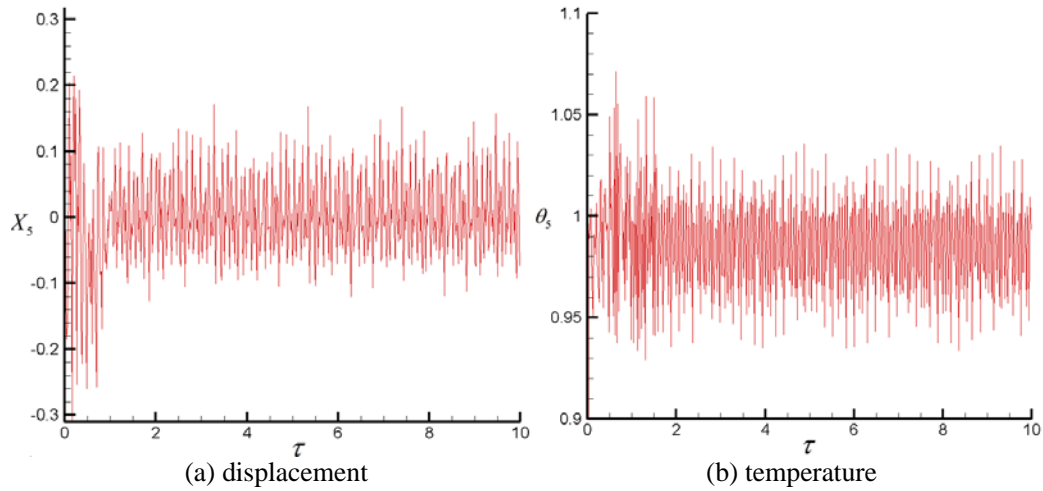


Fig. 11 Liquid slug displacement and vapor temperature ($H_e = H_c = 500$, $A_1 = A_2 = 0$, $A_3 = 0.15$)

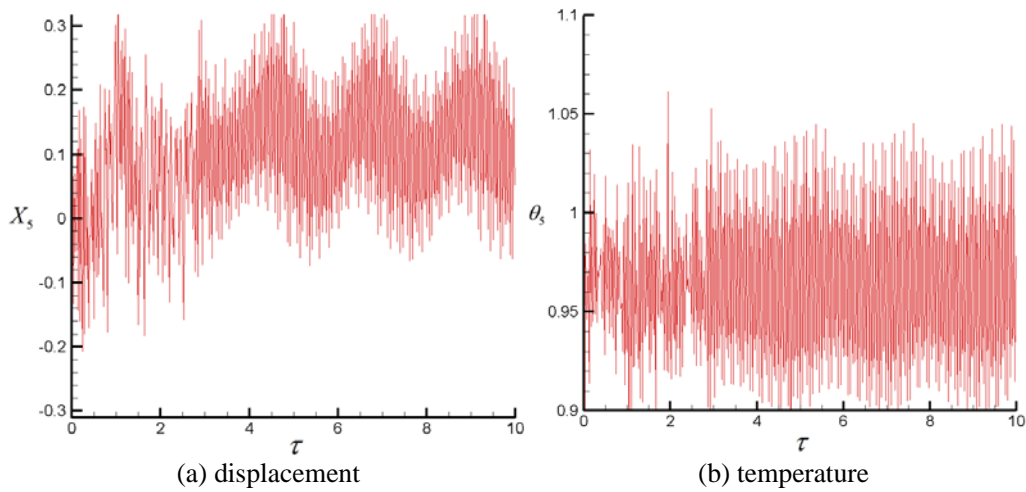


Fig. 12 Liquid slug displacement and vapor temperature ($H_e = H_c = 500$, $A_1 = A_2 = 0.20$, $A_3 = 0.15$)

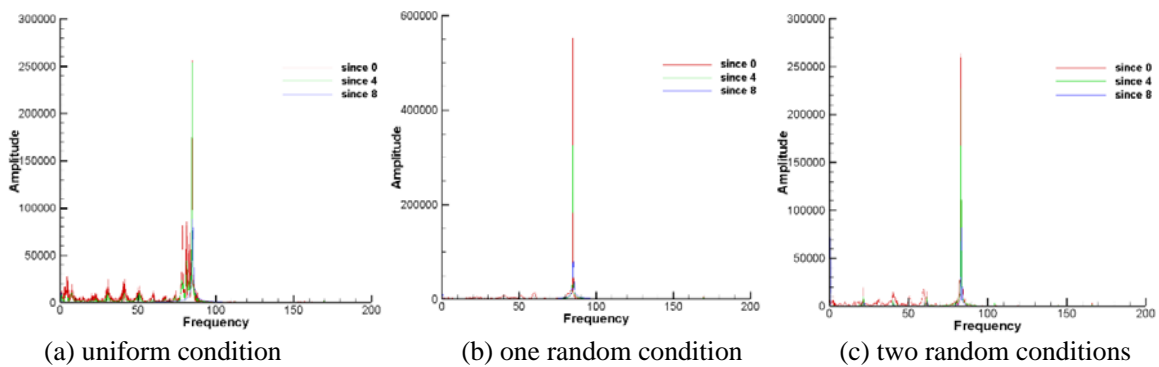


Fig. 13 Comparison of frequencies ($H_e = H_c = 500$)

Figure 13 shows the comparisons of frequencies among the three sets of different initial conditions; Only the one since time equals to 8 is in consideration too. The results for all three cases lead to one main frequency around 75. It means OHPs with different initial conditions reach periodic results with slightly different frequency. Regarding oscillation amplitude and circular frequency together, uniform initial condition leads to the best OHP performance in all three sets of H_e and H_c .

5. CONCLUSIONS

Initial condition effects on the oscillatory flow in OHP are investigated in present work. Uniform initial condition, random initial liquid displacement and random initial vapor temperature, pressure and liquid displacement are in consideration. Three cases with different initial conditions are simulated, respectively. In test case1, the oscillation amplitudes are 0.28, 0.25 and 0.20, and they are 0.30, 0.20 and 0.20 in test case 2. The oscillation amplitudes results in test case 3 are similar to each other while adding two random parameters limits the liquid plug moving region. The frequencies are also compared for all test cases. The results indicate that the non-uniform initial condition may lower the oscillation amplitude and circular frequency in OHP. Setting the initial condition close to uniform one is an efficiency way to better the OHP performance.

ACKNOWLEDGMENT

Support for this work by the U.S. National Science Foundation under grant number CBET- 1066917, Chinese National Natural Science Foundations under Grants 51129602 and 51276118 are gratefully acknowledged.

NOMENCLATURE

A_c	cross sectional area of the tube	(m ²)	x_i	liquid slug displacement	(m)
d	heat pipe diameter	(m)	X	dimensionless liquid slug displacement	(-)
h	heat transfer coefficient	(W/m ² K)	γ	specific heats ratio	(-)
L	length	(m)	ε	charge ratio	(-)
m_v	vapor plug mass	(kg)	θ	dimensionless temperature	(-)
M	dimensionless mass	(-)	μ	viscosity	(kg/ms)
p	pressure	(Pa)	ν	kinematic viscosity	(m ² /s)
P	dimensionless pressure	(-)	τ	dimensionless time	(-)
RN	random number	(-)	τ_p	shear stress	(N/m ²)
T	temperature	(K)	ρ	density	(kg/m ³)

REFERENCES

- [1] Akachi H., "Looped capillary heat pipe, Japanese Patent", No. Hei697147, (1994).
- [2] Miyazaki Y. and Akachi H., "Heat transfer characteristics of looped capillary heat pipe", Proceedings of the 5th International Heat Pipe symposium, pp. 378-383, (1996).
- [3] Miyazaki Y. and Akachi H., Oscillatory in oscillating heat pipe, Proceedings of the 11th International Heat Pipe Conference, pp. 131-136, (1999).
- [4] Hosoda M., Nishio S. and Shirakashi R., "Meandering closed-loop heat-transfer tube", Proceedings of the 5th ASME/JSME Joint Thermal Engineering Conference, pp. 15-19, (1999).
- [5] Qu W. and Ma H., "Theoretical analysis of startup of a pulsating heat pipe", International Journal of Heat and Mass Transfer, 50(11), pp. 2309-2316, (2007).
- [6] Kiseev V. and Zolkin K., "The influence of Acceleration on the performance of oscillating heat pipe", Proceedings of the 11th International Heat Pipe Conference, pp. 154-158, (1999).
- [7] Maezawa S., "Experimental study on chaotic behavior of thermo hydraulic oscillation on oscillating thermosyphon", Proceedings

- of the 5th International Heat Pipe symposium, pp. 131-137, (1996).
- [8] Lee W., Jung H., Kim J. and Kim J., "Flow visualization of oscillating capillary tube heat pipe", Proceedings of the 11th International Heat Pipe Conference, 131-136, (1999).
 - [9] Shafii M., Faghri A. and Zhang Y., "Thermal modeling of unlooped and looped pulsating heat pipes", Journal of Heat Transfer, 123(6), pp. 1159-1172, (2001).
 - [10] Shafii M., Faghri A. and Zhang Y., "Analysis of heat transfer in unlooped and looped pulsating heat pipes", International Journal of Numerical Methods for Heat & Fluid Flow, 12(5), pp. 585-609, (2002).
 - [11] Zhang Y. and Faghri A., "Heat transfer in a pulsating heat pipe with open end", International Journal of Heat and Mass Transfer, 45(4), pp. 755-764, (2002).
 - [12] Zhang Y. and Faghri A., "Oscillatory flow in pulsating heat pipes with arbitrary numbers of turns", AIAA Journal of Thermophysics and Heat Transfer, 17(3), pp. 340-347, (2003).
 - [13] Zhang Y. and Faghri A., "Advances and unsolved issues in pulsating heat pipes", Heat Transfer Engineering, 2008, 29, 1, 20-44.
 - [14] Liang S. and Ma H., "Oscillating motions of slug flow in capillary tubes", International Communications in Heat and Mass Transfer, 31(3), pp. 365-375, (2004).
 - [15] Shao W. and Zhang Y., "Thermally-induced oscillatory flow and heat transfer in an oscillating heat pipe", Journal of Enhanced Heat Transfer, 18(3), pp. 177-190, (2011).
 - [16] Shao W. and Zhang Y., "Effects of film evaporation and condensation on oscillatory flow and heat transfer in an oscillating heat pipe", ASME journal of Heat transfer, 133(4), pp. 042901, (2011).
 - [17] Shao W. and Zhang Y., "Effects of capillary and gravitational forces on performance of an oscillating heat pipe", Frontiers in Heat Pipes, 2(2), pp. 023003, (2011).
 - [18] Kim S., Zhang Y. and Choi J., "Effects of fluctuations of heating and cooling section temperatures on performance of a pulsating heat pipe", Applied Thermal Engineering, 58, pp. 42-51, (2013).
 - [19] Thompson S., Ma H., Winholtz R. and Wilson C., "Experimental investigation of miniature three-dimensional flat-plate oscillating heat pipe", Journal of Heat Transfer, 131(4), pp. 043210, (2009).
 - [20] Ji Y., Ma H., Su F. and Wang G., "Particle size effect on heat transfer performance in an oscillating heat pipe", Experimental Thermal and Fluid Science, 25(4), pp. 724-727, (2011).
 - [21] Loan C., "Computational frameworks for the fast Fourier transform", Society for Industrial Mathematics, (1992).
 - [22] Yang M., Zhou Y., Zhang Y. and Li Z., "Lattice Boltzmann method of simulation of flows with internal slotted hollow", Journal of Thermophysics and Heat Transfer, 28(2), pp. 279-286, (2014).